JOURNAL OF MULTIFUNCTIONAL MATERIALS & PHOTOSCIENCE
11(1), June 2020, pp. 47-64

Preparation of Activated carbon from Coal and their application in the adsorption of heavy metal ions

Zambaga Otgonbayar [1], Won-Chun Oh [1, 2*]

[1]*Department of Advanced Materials Science & Engineering, Hanseo University, Seosan-si, Chungnam, Korea, 356-706*
[2]*College of Materials Science and Engineering, Anhui University of Science & Technology, Huainan 232001, PR China*
**Corresponding author: Won-Chun Oh*, E-mail: wc_oh@hanseo.ac.kr*

Abstract: Activated carbons (ACs) have desirable characteristics that make them attractive for many industrial applications. In order to reduce their production cost, there is always a need to find alternative low-cost feedstock precursors. Nowadays zero-waste technologies play an important role in sustainable development, therefore using of coal by-product as source of AC is strongly recommended. A series of activated carbons was prepared from bituminous coal by chemical activation with potassium hydroxide and zinc chloride and also by physical activation with carbon dioxide. The effect of process variables such as carbonization time, temperature, particle size, chemical agents, method of mixing and impregnation ratio in the chemical activation process was studied in order to optimize those preparation parameters. A number of specialized processes have been developed to the removal of heavy metals from waste discharges and for the remediation of contaminated soils and groundwaters. Technologies described include chemical precipitation (including hydroxide, carbonate, or sulfide reagents), coagulation/flocculation, ion exchange, solvent extraction, extraction with chelating agents, complexation, electrochemical operation, cementation, membrane operations, evaporation, adsorption, solidification/stabilization, and vitrification. Depend on the morphology texture, activation method, the adsorption and removal efficiency of heavy metal are defined.

1. Introduction

There are totally four types of coal. Type refers to steps in a slow, natural process called "coalification, during which buried plant matter changes into an ever denser, drier, more carbon rich, and harder material. There are totally four types have: anthracite, bituminous, subbituminous and lignite. Activated carbons are complex objects which are difficult to classify on the basis behaviour, surface morphology. Mostly, main classification is depending on the particle size, synthesis method, and using application. Totally, there are seven ranks of activated carbonaceous precursor followed by activation of the resulting char in the presence of some activating agents such as carbon dioxide or steam. carbon have which depends on the shape size and application, such as powdered, granular, extruded, bead, impregnated, polymer depends on the shape size and application, such as powdered, granular, extruded, bead, impregnated, polymer and

woven activated carbon. Activated carbon due to its high porosity profile has been widely used in catalytic processes, electrochemistry, adsorbents and for various applications especially in the biomedical and environmental fields. The high porosity and the large surface area, achieved after the activation process, confers very high adsorption capacity to activated carbons, which is difficult to obtain with other sorbents. Consequently, the field of application of an activated carbon is extremely wide. Microporous carbons may be suitable either for gas or vapor adsorption (air purification, gas separation, catalysis, solvent recovery, gasoline emission control, etc.). Meso-macroporous activated carbons are used for liquid phase applications (water and industrial wastewater treatment, food industry, catalyst support etc.). Liquid phase applications account for about 80% of the total activated carbon use.

Basically, there are two different processes for the preparation of active carbon: physical and chemical activation. Physical activation involves carbonization of a carbonaceous precursor followed by activation of the resulting char in the presence of some activating agents such as carbon dioxide or steam. In physical activation, elimination of a large amount of internal carbon mass is necessary to obtain a well-developed carbon structure, whereas in the chemical activation process all the chemical agents used are dehydrating agents that influence pyrolytic decomposition and inhibit formation of tar, thus enhancing the yield of carbon. The temperatures used in chemical activation are also lower than that used in the physical activation process, and therefore the development of a porous structure is better in the case of the chemical process. Activated carbon is a highly porous carbon-based material, which has been subject to an activation process, either with oxidizing gases, such as steam, carbon dioxide, air or a mixture of them (a process called physical activation) and temperature condition was above 250 °C, usually in the temperature range of 600–1200 °C, or by means of chemical agents, such as $ZnCl_2$, H_3PO_4, KOH (a process called chemical activation and used reagents are alkali and alkaline earth metal containing substances). Physical activation of coal and lignocellulosic materials has been extensively studied in the past and chemical activation has been a subject of investigation by a number of workers. Some authors studied the combination of these two methods [1-3] to obtain high surface area adsorbents. In the case of chemical activation, the effects of KOH [4, 5] and $ZnCl_2$, [6-9] on carbonization of coal and other precursors have been of particular interest, and zinc chloride in particular is the widely used chemical agent in the preparation of activated carbon. Modification of AC is considered as an effective process to enhance its adsorptive characteristics. The KOH activated carbons prepared from elm tree waste were treated by a novel and green method using thermal tension by successive washing with 80/ °C, 95 °C and 2 °C water to enhance the pore development and adsorption of Cr (VI) and Pb (II) from aqueous solutions. The simulation of thermal stress using a finite-element-analysis implied that the quick temperature changes might cause the formation of cracks leading to enhancement of porosity. The nature of the precursor material, synthesis method, and activation conditions are the most important factors that can affect the characteristics of ACs including surface area, pore volume, and size distribution [10] (as shown in **Table 1**). The pore size distribution is used to categorize ACs into micro-,

meso- and macroporous, and indicates the degree of heterogeneity in the ACs structure [11]. Various modification methods of carbonaceous materials can also enhance their pore structure and surface chemistry by introducing the non carbon moieties to the surface of porous materials which improves their affinities to specific sorbates and consequently enhances adsorption performance of AC for wastewater treatment. Surface modification of ACs through creating surface oxygen functional groups like carbonyl groups can be performed through dry and wet oxidations. Reactions of oxidation gases like steam and CO_2 with surface of AC at high temperatures (respectively 700 and 800 °C) [12] is called dry oxidation while wet oxidation is reactions of oxidizing solutions like nitric acid (at 120 °C) [13] and ammonium per sulphate under moderate temperature [14] or hydrogen peroxide at room temperature [15]. Basic treatment of AC with NaOH solution (at 30 °C) or gaseous ammonia thermal treatment (at 300 °C) enhanced the adsorption efficiency of organic and mineral pollutants from wastewater [16]. Generally, most of post-AC treatments are based on the use of chemicals or high temperatures. In the present study, a novel and green process, without the use of chemicals, was proposed for post-modification of potassium hydroxide (KOH) activated carbon prepared from elm tree lignocellulosic.

Table 1.Comparison of gas activation and chemical activation

	Preparation condition	
	Gas	Chemical
Raw material	Carbonized and dried compounds	Carbonized and non-carbonized compounds
Activation agents	Water vapor, CO_2, O_2	$ZnCl_2$, H_3PO_4, NaOH
Activation temperature	750~1150°C	400~800°C
Activation system	Easy, friendly environmental	Complex, corrosion, non-friendly environmental
	Properties	
Pore volume (ml/g)	0.45~1.30	0.70~1.90
Surface area (m^2/g)	700~1600	700~1800
Average pore size (+!)	10~30	10~35
	Application	
	Gas ads., deodar, air purification, solvent recovery, catalyst support, wastewater purification	Decolorization, deodar, pharmaceuticals, surgery purification, liquor, petroleum, wastewater purification

Methodology of Manufacturing and Synthesis of Activated carbon

The synthesis method of activated carbon categorized in two pathways: chemical and physical (gas). **Figure 1** shows the typical physical (gas) and chemical activation process. The powdered activated carbons were produced from lignocellulosic waste by chemical activation with KOH. Preparing a mixture of raw material and KOH were done according to the methods reported for grape seeds [17]. Based on literature, relatively high carbonization temperature [18] and impregnation ratio [19] in KOH activation method resulted in more micro-porosity of prepared AC. Therefore, 10 g of the lignocellulosic waste of elm tree was mixed with 20 g of powdered KOH for 24 h in ambient temperature by impregnation ratio of 2:1 (activating agent: lignocellulosic waste). The prepared impregnated samples were put in a stainless-steel crucible and pyrolyzed for 1 h in a muffle furnace. The atmosphere was neutralized by N_2 gas flow at a constant

rate of 1 L min. The carbonization temperature was adjusted at 800 °C KOH activation method with a heating rate of approximately 10 °C min. The sample was cooled up to ambient temperature under N_2 atmosphere and the produced activated carbon was weighted. After impregnation of raw materials and KOH the structure of biomass (i.e. cellulose) will break down. Then the chemical activator dehydrates the raw materials during pyrolysis in the absence of air. As a result, the carbon skeleton is charred and aromatized, which will finally create a porous structure.

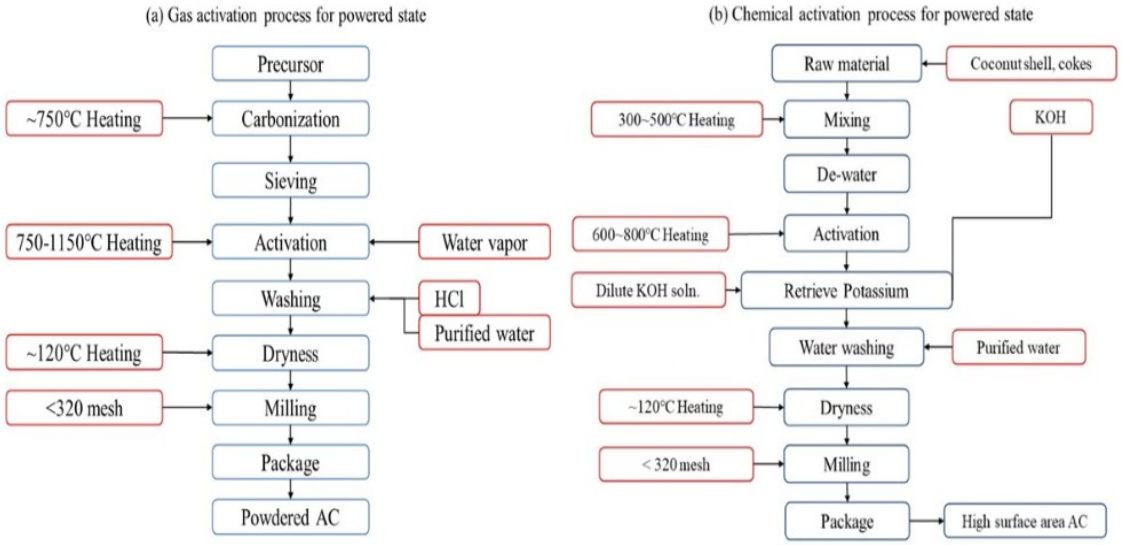

Figure 1. Typical activation process of Activated carbon.

2.1 *Method of heavy metal removal*

A number of specialized processes have been developed for the removal of heavy metals from waste discharges and for the remediation of contaminated soils and groundwaters. For the removal of metals from solution, these unit operations involve chemical precipitation (hydroxide, carbonate, sulfide, or combinations thereof), coagulation/ flocculation, ion exchange, solvent extraction, cementation, complexation, electrochemical operations, evaporation, filtration, and membrane processes. Several reviews are found in the technical literature that summarize the various physical/ chemical treatments for heavy metal removal [20, 21].

i. ***Chemical precipitation*** - transforming a soluble compound into an insoluble form through the addition of chemicals, such that a supersaturated environment exists (i.e., the solubility product is exceeded) (as shown in **Figure 2a**). Chemical precipitation is a complex phenomenon resulting from the induction of supersaturation conditions• Precipitation proceeds through three stages: (1) nucleation, (2) crystal growth, and (3) flocculation.

ii. ***Coagulation/Flocculation -*** is capable of removing heavy metals from solution. Coagulation refers to charge neutralization of the particles (as shown in **Figure**

2b). Flocculation involves slow mixing to promote agglomeration of the destabilized particles.

iii. *Ion Exchange* - removal of heavy metals is accomplished by the exchange of ions on the resin for those in wastewater (as shown in **Figure 2c**). Ion exchange is an ideal method for removal of trace amounts of impurities from dilute wastewaters, with the high quality treated water ready for reuse. Because ion exchange is efficient in removal of dissolved solids from normally dilute spent rinse waters, it is well suited for use in water purification and recycle.

iv. **Flotation** - depends on the use of a surfactant that causes a non-surface active material to become surface-active, forming a product that is removed by bubbling gas through a bulk solution to form a foam (as shown in **Figure 2d**).

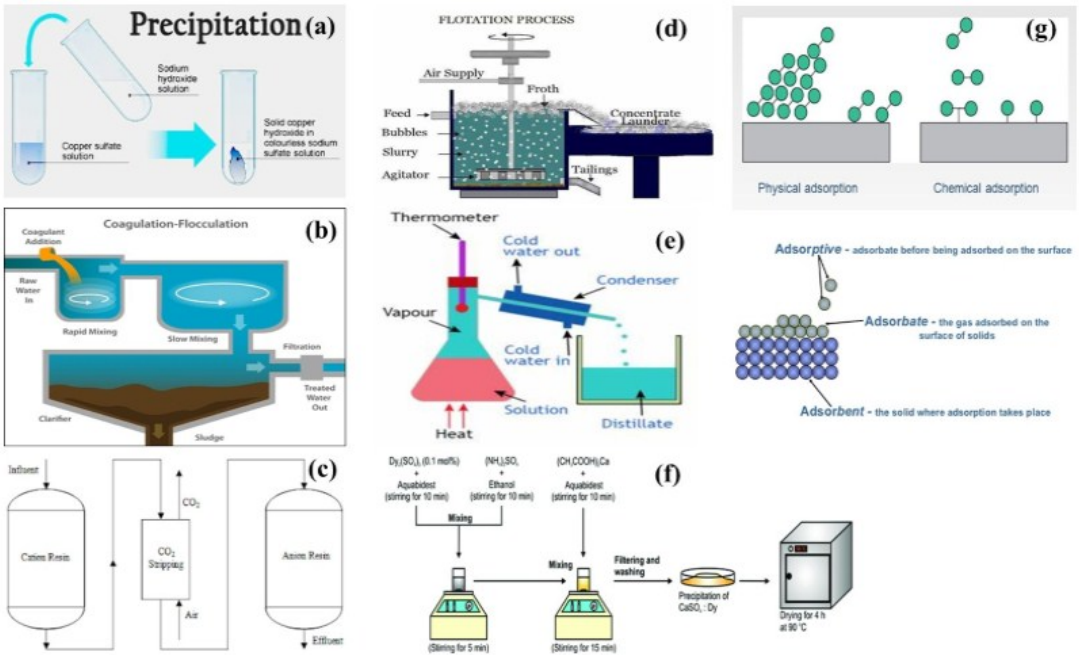

Figure 2. Schematic illustration of Method of heavy metal removal.

v. **Electrochemical operations** - a direct current is passed through an aqueous solution containing metal ictus between cathode plates and insoluble amides. The positive charged metallic ions adhere to the negatively charged cathodes, leaving a metal deposit that can be stripped off and recovered. The theory of operation basically involves an oxidation-reduction reaction whereby electrons are supplied by an external electrical source, reducing the metal ions in the electrolyte to form elemental metal at the cathode surface.

a. Cathode: $Cu^{2+} + 2e^{-} = Cu^{0}$ (1)

b. Anode: $H_2O - 2H^{+} + O_2 + 2e^{-}$ (2)

vi. **Evaporation/Distillation** - treatment has been for product recovery, with some limited use to treat final concentrated wastewater residues to dryness. These techniques are basically end-of-the-pipe processes (as shown in **Figure 2e**). This technique requires sorting of wastes by types and use of various means for exclusion and or removal of impurities.

vii. **Coprecipitation/ Adsorption** - when a solid phase is precipitated from solution, impurities that are normally soluble under the conditions of the precipitation may adsorb onto nuclei or crystals and be removed with the parent solid as a single phase (as shown in **Figure 2f**). There are several type of adsorption methods has: such as surface adsorption, occlusion, isomorphic inclusion, mechanical entrapment, post precipitation. There are five basic techniques that can be used to remove heavy metals from solution. These techniques include formation of metal hydroxides (heavy metals are removed by adding an alkali), metal carbonates (using soda ash-sodium carbonate), metal sulfides, and xanthate treatment (xanthate acts as an ion exchange materials removing heavy metals and replacing them with sodium and magnesium), or combinations (the chemical treating agents (precipitants) from more than one of the previous chemical precipitation systems are combined) thereof.

viii. **Adsorption** - characteristics of cationic and anionic species onto activated carbon surfaces. Important physical/chemical properties affecting inorganic electrolyte adsorption include specific surface area, pore structure, electrophoretic properties, and surface acidity (**Figure 2g**). The rule of anions in the adsorption of heavy metals was delineated by consideration of the following reaction steps: (1) anions accumulate in the double layer of a positively charged particle, (2) approach of metal ions to the soil surface is facilitated, and (3) complexes form between the heavy metal ions and the already adsorbed aqueous anionic ligands .

Result and discussion

The adsorption capacity of activated carbon depends upon porosity as well as the chemical reactivity of functional groups at the surface [22]. The main types of atoms which can bond to the edge of the carbon layers and have significant effects on the surface properties are oxygen, nitrogen, halogen, and hydrogen [23]. Therefore, the FTIR spectroscopy method was used to obtain information about the presence of possible functional groups on the surface of ACs (**Figure 3**). The FTIR spectrum of the ACs derived from elm wood treated with or without thermal tension treatment had many similar features. However, some different intensities of the peaks were identified. The wide peak between 3100 and 3600 cm^{-1} belongs to the phenolic, alcoholic, and carboxylic acid –OH groups [24, 25], which is the most responsible for heavy metal ions adsorption in lignocellulose materials. The peak in the range of 2800–2900 cm^{-1} indicated the presence of –CH group in carboxylic acids, methyl, or methylene [26]. The intensity of this peak in thermal tension treated AC was higher than non-treated AC and hence showed a higher adsorption capacity (which will be discussed further). The peak located at 1600 cm^{-1} indicated C=C stretching of the aromatic rings. At high carbonization

temperatures, C-H bond may decompose to form a more stable aromatic C=C bonds. This might also be as a result of the conjugation of C=O groups with aromatic rings and formation of carbonyl-containing groups [27]. **Table 2** shows the elemental analysis result of Activated carbon which obtained with the chemical activation using NaCl, $CaCl_2$, KCl, and H_3PO_4 (i.e., samples C-Na, C-Ca, C-K and C-P, respectively) showed the highest content of oxygen, which could be attributed to the introduction of oxygenated functional groups (acidic, basic and neutral) that modify the surface chemistry and adsorption properties [28-31]. The pyrolyzed sample C showed a lower oxygen content than those obtained with CO_2 activation (samples C-CO_2). The activated carbon obtained from H_3PO_4 treatment (sample C-P) showed the highest surface acidity. The morphology structure, functional group, and specific surface area of the Activated carbon with additional element/compound are main factor of adsorbent material. For example, zeolite combined with activated carbon showed a high adsorb abilities of Cu^{2+} could reach up 92.8%. A composite structure of the zeolite and activated carbon is successfully synthesized through CO_2 activation followed by the hydrothermal synthesis method using coal gangue as the raw material. The specific surface area of a so-prepared composite is 669.4 m^2/g, which is much larger than that of the pure NaA type zeolite (249.3 m^2/g). **Figure 4** shows the morphological and structural property of adsorbent material. From the low magnification (Figure 4a), the zeolites have a good dispersive property, uniform size distribution and regular geometrical shapes without impurity on a large scale, indicating that the carbon element has been burned out completely. From the high magnification (Figure 4b), the single zeolite is a regular hexahedron with each side about 1.5–2 ìm in length. Each of them has an angular shape and a smooth surface. Some irregular bulk materials appear in this sample and more and more zeolites grow on the surface of these bulk materials to form larger aggregates in Figure 4 (c-d). The zeolite surface becomes rougher in a system with many carbon-based materials. According from TEM image, the activated carbon has a disordered and fluffy structure containing many big pores. The inset image between Figure 4e and f is the SAED pattern of ZAC. The main object in the image is a dispersed diffraction ring, which is ascribed to the amorphous structure of activated carbon. The SAED pattern also exists many irregular diffraction spots, illustrating that there exists polycrystalline phase.

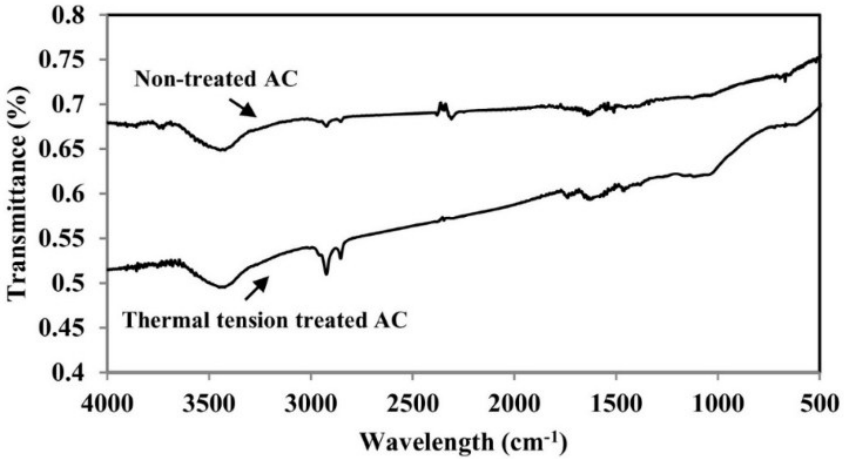

Figure 3. FTIR spectra of prepared activated carbons prepared from the lignocellulosic waste of elm tree [28].

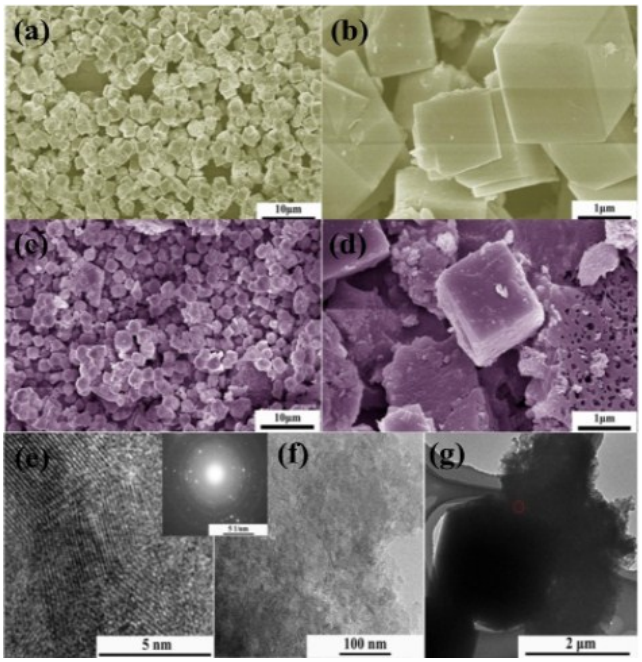

Figure 4. SEM images of zeolites containing different contents of carbon (a-b) Zeolite, (c-d) ZAC (zeolite with activated carbon), (e) A high resolution TEM image of zeolite in ZAC. (f) A high magnification TEM image of activated carbon in ZAC.(g) low magnification TEM image of ZAC.

Table 2. Results of elemental analysis and textural properties of adsorbents obtained from pecan nutshell biomass.

	Elemental analysis, %					Textural parameters [a]				
Sample	N	C	H	O	p.z.c.	S_{BET} m^2/g	V_t cm^3/g	V_{mic} cm^3/g	V_{mes} cm^3/g	AP Á
C-Na	0.510	78.827	0.576	20.087	9.15	786	0.614	0.474	0.140	30.79
C-Ca	0.347	68.961	0.774	29.919	9.25	490	0.399	0.266	0.133	31.75
C-K	0.362	76.465	0.879	22.294	9.38	808	0.546	0.374	0.172	26.72
C-CH	0.273	82.159	0.790	16.778	7.45	365	0.200	0.186	0.014	21.07
C-S	0.140	81.351	0.861	17.647	6.88	310	0.163	0.160	0.002	20.11
C-P	0.231	68.330	0.842	30.597	2.86	396	0.208	0.206	0.002	20.20
C-CO_2	0.126	80.906	0.636	18.333	7.87	377	0.215	0.190	0.024	22.01
C	0.063	83.598	0.773	15.565	9.43	331	0.171	0.167	0.003	19.56

3.1. Thermal tension treatment of activated carbon

For thermal tension treatment, the obtained AC were stirred three times at 80 °C for 3 h in distilled water until the pH was attained 6–7. The use of hot water during washing is aimed to dissolve and extract the rests of activating agent and retained tars in order to free the porous texture developed during the activation process. This washing process is favored at high temperature, and thus 80 °C was selected [32]. In order to expose the sample to thermal stress (temperature change), 1/ L of boiling distilled water (95 °C) and subsequently 1/ L of cold distilled water (2 °C) were immediately passed through each sample. To confirm the effectiveness of thermal tension on the textural development

and adsorption capacity of prepared AC, the sample was also washed without any thermal treatment. In this method, the sample was sequentially washed with distilled water in ambient temperature until the filtrate reached to pH of 6–7. The obtained ACs were dried in an oven, left in the desiccator until became cool and then kept in separate containers for subsequent use. The simulation is generally based on the mechanical and thermal properties of the material such as Young's modulus, Poisson's ratio, density, expansion coefficient, specific heat, effective thermal conductivity, and heat transfer coefficient [33]. This simulation consisted of two coupled temp-displacement (Transient) steps with a time of 0.05 s. The initial temperature of the object was 80 °C. In the first step, the temperature of boiling water was 95 °C, and in the second step, it was 2 °C. It was also assumed that all cube faces were in contact with water. It should be noted that due to the small size of the selected material, the temperature changes could be occurred quickly at a short time. **Figure 5** shows the temperature gradient and thermal stress gradient in the cut view of cube during the time, respectively. After treating AC at 80 °C, in the first step of thermal stress (Figure 5), at time t = 0, the temperature of the particle is at 80 °C. By adding water at 95 °C to AC, the particle temperature increases in a fraction of a second. As time passes, the temperature difference arises between the surface and the middle of the particle. After that, at $t = 6.7 \times 10^{-3}$ s, the whole particle is at 95 °C. In the second step (Figure 5), the temperature of a particle at 95 °C (t = 0), decrease quickly and reaches 2 °C in a fraction of a second ($t = 2.7 \times 10^{-2}$ s) after adding cold water. The thermal stress and the fractures are recognizable by the temperature gradient in the outer, middle, and internal layers of the particle, during washing with hot water at 95 °C, then cold water at 2 °C. The AC undergoes considerably lower stresses in the first step comparing to the second step. At time t = 0, there is no temperature gradient and the stress in the particle is zero. In the first step, according to the temperature change from 80 °C to 95 °C, the thermal stresses reach to 0.592 MPa. In the second step, in which the temperature change is higher than the first step (from 95 °C to 2 °C), the thermal stress levels reach the maximum (2.937 MPa). As the mechanical properties of material including the strength and elasticity, the thermal properties, and the corrosion resistance are affected by the amount of porosity in a material [34], the performance of thermal shock may be more efficient in the AC with high porosity and surface area.

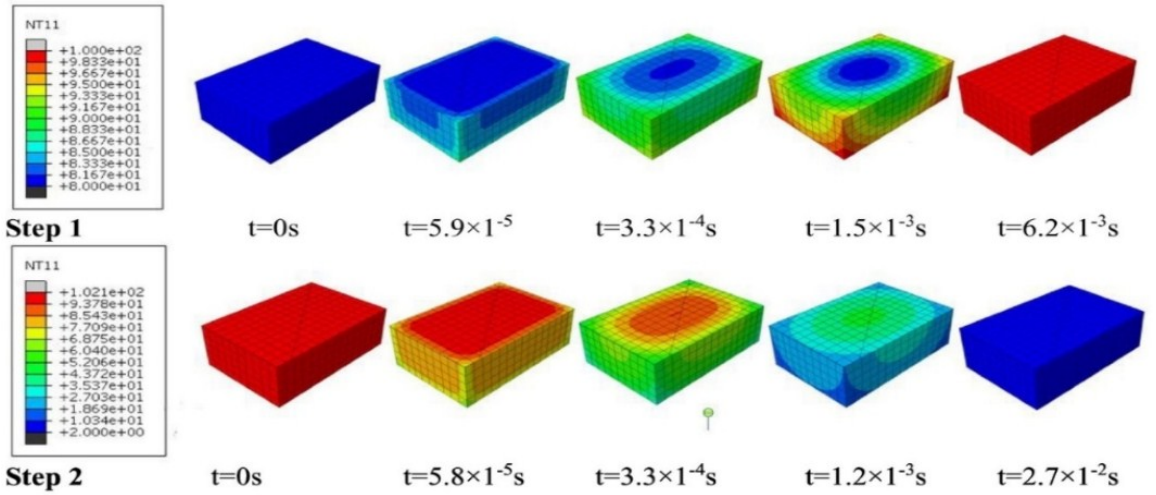

Figure 5. Temperature change gradient during thermal tension treatment of the prepared activated carbon, step 1: temperature change from 80 °C to 95 °C, step 2: temperature change from 95 °C to 2 °C [28].

3.2. *Adsorption property of Activated carbon material*

The heavy metal pollution has become an increasingly serious environmental problem due to the threat of living species and ecological security with the continuous growth of population and the rapid development of the global industry [35, 36]. Heavy metal pollution caused by cadmium, chromium, copper, lead, mercury, nickel and arsenic is most serious to the human body [37]. There are several adsorbent materials such as zeolites [38], polymers [39-44], fly ash [45], biomasses [46-52], graphene oxide [53-55], and activated carbon [56] which have been applied for the removal of heavy metals. Among them, AC is a considerable adsorbent material due to Textural properties (i.e., surface area and pore distribution) and surface chemistry (e.g., functional groups) are key point to establish the adsorption property of the adsorbent. **Figure 6** shows the adsorption capacities of pecan-based adsorbents for the removal of heavy metal ions Cu^{2+}, Cd^{2+}, Ni^{2+} and Zn^{2+}. Metal adsorption capacities in mono-component studies ranged from 0.011 to 0.368 mmol/g and the highest values were obtained for the removal of Cu^{2+} and Zn^{2+} ions. Overall, activated carbons C-Na, C-Ca and C-K showed the best removal behavior for tested heavy metal ions, while the activated carbon C-S showed the lowest adsorption capacities at tested operating conditions. Therefore, it is clear that the chemical activation may improve the metal adsorption properties of the adsorbent obtained from single pyrolysis up to 12.14% using a proper route and chemical reagent. **Figure 7** illustrates the mechanism proposed for heavy metal removal using pecan nutshell – based adsorbents. Heavy metal ions may interact with the oxygenated functional groups of the adsorbents besides the calcium present in the adsorbent surface can be exchanged with these ions. In particular, the activation procedures increased the ion exchange properties of these adsorbents. This mechanism also explains the antagonistic adsorption in multi-metallic solutions where the adsorption capacities decreased with the increments of initial concentrations of binary solutions. The chemical activation may improve the metal adsorption properties of these adsorbents up

to 1214 %. Activated carbons obtained with a chemical activation using NaCl and KCl showed the highest surface area and the best calcium exchange properties for heavy metal adsorption. Furthermore, the pH condition is side factor for the heavy metal removal efficiency. The effect of optimum pH of lead (Pb^{2+}), copper (Cu^{2+}), chromium (Cr^{3+}), cadmium (Cd^{2+}) solutions were 2.10, 2.08, 2.09, and 2.13, respectively. Generally, the pH value of the heavy metal solution increased with bamboo activated carbon dosage. **Table 3** demonstrates the effects of Mosso and Ma bamboo activated carbons (soaking time 24 h) on the adsorption capacity and removal efficiency of heavy metal ions (10 ppm). The pH values of the test heavy metal solutions were 2.47–2.54. The adsorption capacity increased rapidly with increasing pH value in the initial stage. However, the adsorption capacity decreased with increasing pH value after the maximum adsorption capacity was reached. The corresponding pH value defined as the optimum pH value was obtained when the maximum adsorption capacity was reached. Table 4 also shows 100% removal efficiency by the S1C1 and S2C1 groups on Pb^{2+} and Cu^{2+}, and by the S1M1 and S2M1 groups on Pb^{2+}, Cu^{2+}, Cr^{3+}, and Cd^{2+}; whereas, a 43.9–65.8% removal efficiency by the S1C1 group on Cr^{3+} and Cd^{2+}, and the S2C1 group on Cd^{2+} was observed. The optimum pH values of Mosso and Ma bamboo activated carbons for maximum removal efficiency were 7.26–7.86 and 7.53–9.82, respectively. Ücer et al. (2006) reported that the optimum pH values of tannic acid immobilized activated carbons for adsorption of Cu^{2+}, Cd^{2+}, Zn^{2+}, Mn^{2+}, and Fe^{3+} were 5.4, 5.7, 5.6, 5.4, and 4.0, respectively. When activated carbon prepared from apricot stone with a pH value ranging from 1 to 6 was used, the adsorption capacity decreased from 34.70 to 7.86 mg/g for Cr^{6+}; whereas, the adsorption capacity increased from 7.74 to 30.07 mg/g for Cd^{2+}, from 2.83 to 29.47 mg/g for Cr^{3+}, from 2.51 to 27.21 mg/g for Ni^{2+}, from 4.86 to 24.21 mg/g for Cu^{2+}, and from 6.69 to 22.85 mg/g for Pb^{2+}, respectively [55]. In their study, the maximum removal efficiency and corresponding optimum pH value were 99.99% and 1 for Cr^{6+}, 99.86% and 3 for Pb^{2+}, 99.67% and 5 for Cd^{2+}, 99.17% and 6 for Co^{2+}, 98.56% and 4 for Cr^{3+}, 97.59% and 4 for Ni^{2+}, and 96.24% and 4 for Cu^{2+}, respectively. From the above-mentioned references, it was concluded that the adsorption capacity of heavy metal ions by most of the various activated carbons was better at a pH value less than 7.

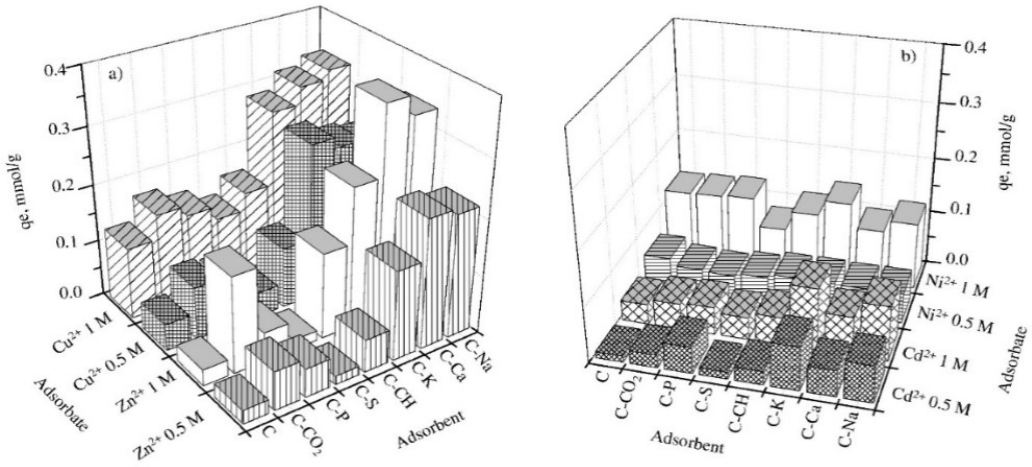

Figure 6. Mono-component adsorption capacities of the pecan-based adsorbents for the removal of heavy metal ions at pH 5 and 30 °C. Heavy metals: a) Cu^{2+} and Zn^{2+}, b) Ni^{2+} and Cd^{2+}.

Table 3. Adsorption capacity and removal efficiency of heavy metal ions by Mosso and Ma bamboo activated carbons (soaking time 24 h).

Bamboo AC	Dosage (g)	Pb (II)			Cu (II)			Cd (II)		
		pH	Adsorption capacity (mg/g)	Removal efficiency (%)	pH	Adsorption capacity (mg/g)	Removal efficiency (%)	pH	Adsorption capacity (mg/g)	Removal efficiency (%)
S1C1	0	2.54	-	-	2.48	-	-	2.54	-	-
	0.1	3.94	0.236	24.26	2.90	0.002	0.10	2.66	0.02	0.01
	0.3	6.07	0.675	99.87	5.81	0.587	86.43	5.90	0.197	29.91
	0.5	7.54	0.407	100.0	7.39	0.401	100	7.26	0.174	43.86
S2C1	0	2.54	-	-	2.48	-	-	2.54	-	-
	0.1	3.66	0.380	20.16	2.99	0.259	14.16	3.24	0.041	2.08
	0.3	7.04	0.638	100.0	6.73	0.660	99.10	6.38	0.238	37.17
	0.5	7.40	0.396	100.0	7.91	0.400	100.0	7.52	0.257	65.83
S1M1	0	2.54	-	-	2.48	-	-	2.54	-	-
	0.1	9.18	1.901	100.0	8.16	1.908	100.0	7.10	0.403	21.02
	0.3	9.70	0.676	99.98	9.25	0.650	100.0	9.77	0.670	98.44
	0.5	10.02	0.404	100.0	9.60	0.634	100.0	9.8	0.398	100.0
S2M1	0	2.54	-	-	2.48	-		2.54	-	-
	0.1	7.83	1.998	100.0	7.10	1.425	73.98	6.95	0.381	20.82
	0.3	7.85	0.667	100.0	8.00	0.650	100.0	7.78	0.655	99.86
	0.5	7.95	0.397	100.0	8.26	0.398	100.0	8.05	0.396	100.0

To improve the adsorption capacity, recent studies have been focused on supporting Fe_3O_4 nanoparticles onto AC. By impregnating Fe_3O_4 nanoparticles into activated carbon, the characteristics of the resulting surface have modified so that there are a large number of active sites that can increase the chemisorption. In particular, Fe_3O_4 nanoparticles-loaded activated carbon can be separated by using an external magnet. The modification of activated carbon chemistry has been developed to increase the number of acidic sites in the surface. It is demonstrated that the presence of functional groups containing oxygen atoms onto AC play a vital role for removal of heavy metals because these groups can form complex with heavy metals [57-59]. Furthermore, the ultrasonic method can accelerate the separation of the heavy metals from polluted water. Carbon materials were doped with magnetic nanoparticles magnetic particles such as Fe, Co, Ni and Cu, especially Fe_3O_4, because of their excellent magnetic properties, wide availability, low cost, and biocompatibility. The synthesis of Fe_3O_4 NPs@AC@$C_4H_8SO_3H$, the growth of Fe_3O_4 nanoparticles and the loading of $C_4H_8SO_3H$ onto AC are shown in **Scheme 1**. Furthermore, the efficient nano-sorbents and nanocatalysts based on metal oxides nanoparticles (MO-NPs) generally include manganese, iron, aluminum, silicon, titanium, and cerium oxides. The interests in these MO-NPs are mainly focused on their high surface areas, reactive functional groups, good selectivity and high metal up-take capacity removal of investigated heavy metal ions [60, 61]. The removal performance of lead (^{22}), cadmium (^{22}) and copper (^{22}) ions on SnO_2-NPs-AC-MnO_2-NPs was investigated and optimized by the batch adsorption technique and applying a number of controlling parameters as pH of contact solution, shaking time, nano sorbent dosage, ionic metal concentration and interfering species. The maximum metal up-take capacities were 4100, 2600 and 2500 ì mol g^{-1} for copper (^{22}), lead (^{22}) and cadmium (^{22}), respectively by applying concentration of Cu(II), Cd(II) and Pb(II) (0.2 mol L^{-1}), time of reaction (30 min), pH 7 of reaction solution.

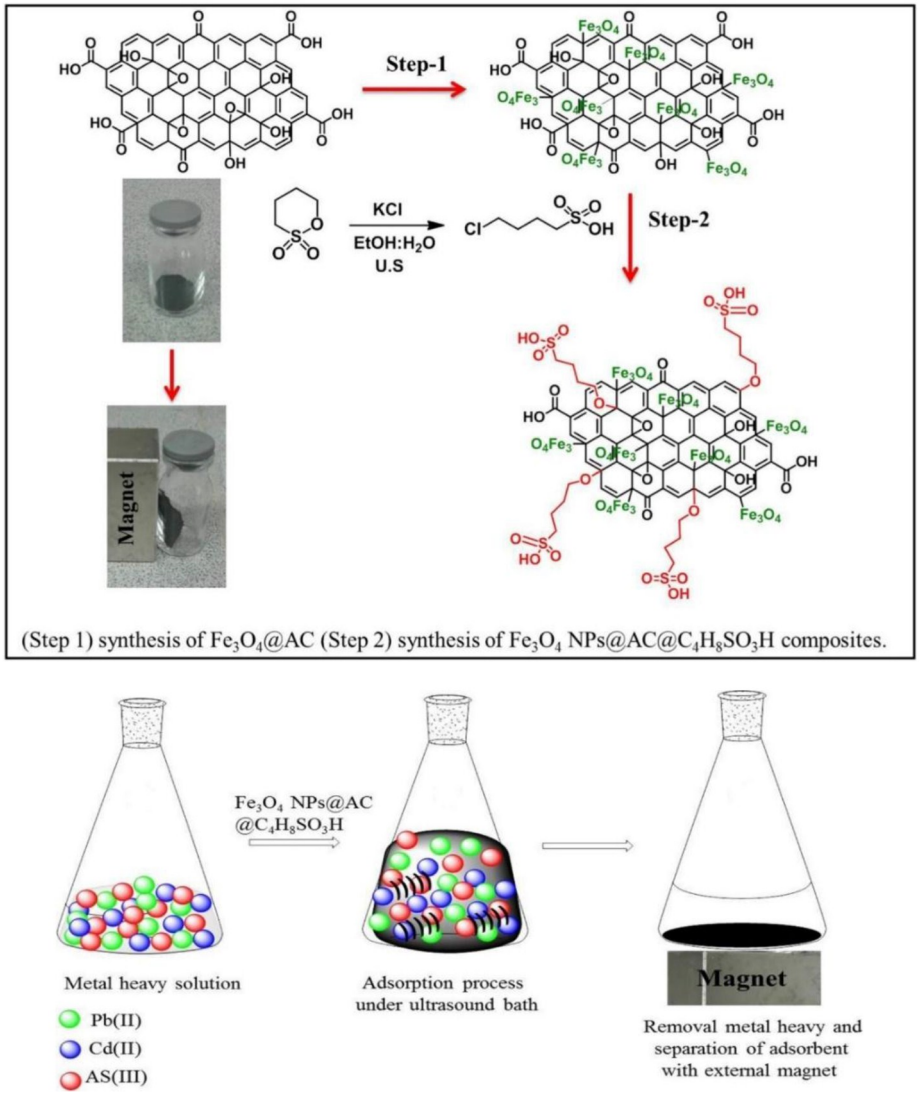

Scheme 1. Synthesis processes and the structure of Fe_3O_4 NPs@AC@$C_4H_8SO_3H$ composites

Conclusion

Activated carbons (ACs) have desirable characteristics that make them attractive for many industrial applications. In order to reduce their production cost, there is always a need to find alternative low-cost feedstock precursors. A series of activated carbons was prepared from bituminous coal by chemical activation with potassium hydroxide and zinc chloride and also by physical activation with carbon dioxide. The effect of process variables such as carbonization time, temperature, particle size, chemical agents, method of mixing and impregnation ratio in the chemical activation process was studied in

order to optimize those preparation parameters. A number of specialized processes have been developed to the removal of heavy metals from waste discharges and for the remediation of contaminated soils and groundwaters. Depend on the morphology texture, activation method, the adsorption and removal efficiency of heavy metal are defined. Nowadays, the surface and texture modification of activated carbon become a considerable research field.

Reference

1. Molina-Sabio M., Reinoso F.R., Buss G.Y., Caturla F. (1989). THE PREPARATION OF ACTIVE CARBONS FROM COAL BY CHEMICAL AND PHYSICAL ACTIVATION, European Patent 0329251.
2. Caturla F., Molina-Sabio M., Rodríguez-Reinoso F. (1991). Preparation of activated carbon by chemical activation with $ZnCl_2$, Carbon, 29, p. 999-1007. https://doi.org/10.1016/0008-6223(91)90179-M
3. Rodríguez-Reinoso F., Molina-Sabio M. (1992). Activated carbons from lignocellulosic materials by chemical and/or physical activation: an overview, Carbon, 30, pp. 1111-1118. https://doi.org/10.1016/0008-6223(92)90143-K
4. Laine J., Calafat A. (1991) Factors affecting the preparation of activated carbons from coconut shell catalyzed by potassium, Carbon, 29, pp. 949-953. https://doi.org/10.1016/0008-6223(91)90173-G
5. Yehaskel A. (1978) (2nd edition), Activated Carbon, Manufacture and Regeneration, Woyes Data Corporation, NJ.
6. Caturla F., Molina-Sabio M., Rodríguez-Reinoso F. (1991). Preparation of activated carbon by chemical activation with $ZnCl_2$, Carbon, 29, p. 999-1007. https://doi.org/10.1016/0008-6223(91)90179-M
7. Ibarra J.V., Moliner R., Palacios J.M. (1991). Catalytic effects of zinc chloride in the pyrolysis of Spanish high sulphur coals, Fuel, 70, pp. 727-732. https://doi.org/10.1016/0016-2361(91)90069-M
8. Kirubakaran C.J., Krishnaiah K., Seshadri S.K. (1991). Experimental study of the production of activated carbon from coconut shells in a fluidized bed reactor**,** Ind. Eng. Chem. Res., 30, pp. 2411-2416. https://doi.org/10.1021/ie00059a008
9. Yanik J., Saglam M., Üstün G., Yüksel M. (1992). Effects of $MgCl_2$ and $ZnCl_2$ additives on the porosity of formed coke, Fuel, 71, pp. 712-713. https://doi.org/10.1016/0016-2361(92)90178-Q
10. Danish M, Ahmad T. (2018). A review on utilization of wood biomass as a sustainable precursor for activated carbon production and application, Renew. Sust. Energ. Rev., 87, pp. 1-21. https://doi.org/10.1016/j.rser.2018.02.003
11. Savova D., Apak E., Ekinci E., Yardim F., Petrov N., Budinova T., Razvigorova M., Minkova V. (2001). Biomass conversion to carbon adsorbents and gas, Biomass Bioenergy, 21, pp. 133-142. https://doi.org/10.1016/S0961-9534(01)00027-7
12. Pallarés J., González-Cencerrado A., Arauzo I. (2018). Production and characterization of activated carbon from barley straw by physical activation with carbon dioxide and steam, Biomass Bioenergy, 115, pp. 64-73. https://doi.org/10.1016/j.biombioe.2018.04.015
13. Abussaud B., Asmaly H.A., Ihsanullah., Saleh T.A., Gupta V.K., Laoui T., Atieh M.A. (2016). Sorption of phenol from waters on activated carbon impregnated with iron oxide, aluminum oxide and titanium oxide, J. Mol. Liq., 213, pp. 351-359. https://doi.org/10.1016/j.molliq.2015.08.044
14. Yang T., Hu X., Zhang P., Chen X., Wang W., Wang Y., Liang Q., Zhang Y., Huang Q. (2019). Study of pre-treatment of quinoline in aqueous solution using activated carbon made from low-cost agricultural waste (walnut shells) modified with ammonium persulfate, Water Sci. Technol., 79, pp. 2086-2094. https://doi.org/10.2166/wst.2019.206
15. Xue Y., Gao B., Yao Y., Inyang M., Zhang M., Zimmerman A.R., Ro K.S. (2012). Hydrogen peroxide modification enhances the ability of biochar (hydro char) produced from hydrothermal carbonization

of peanut hull to remove aqueous heavy metals: batch and column tests, Chem. Eng. J., 200–202, pp. 673-680. https://doi.org/10.1016/j.cej.2012.06.116

16. Vu M.T., Chao H.P., Van Trinh T., Le T.T., Lin C.C., Tran H.N. (2018) Removal of ammonium from groundwater using NaOH-treated activated carbon derived from corncob wastes: batch and column experiments, J. Clean. Prod., 180, pp. 560-570. https://doi.org/10.1016/j.jclepro.2018.01.104
17. Okman I., Karagöz S., Tay T., Erdem M. (2014) Activated carbons from grape seeds by chemical activation with potassium carbonate and potassium hydroxide, Appl. Surf. Sci., 293, pp. 138-142. https://doi.org/10.1016/j.apsusc.2013.12.117
18. Wei M., Yu Q., Mu T., Hou L., Zuo Z., Peng J. (2016). Preparation, and characterization of waste ion-exchange resin-based activated carbon for CO_2 capture, Adsorption, 22, pp. 385-396. https://doi.org/10.1007/s10450-016-9787-8
19. Foo K.Y., Hameed B.H. (2012). Microwave-assisted preparation, and adsorption performance of activated carbon from biodiesel industry solid reside influence of operational parameters, Bioresour. Technol., 103, pp. 398-404. https://doi.org/10.1016/j.biortech.2011.09.116
20. Dean J.G., Bosqui F.L., Lanouette K.H. (1972). "Removing Heavy Metals from Wastewater", Environ. Sci. Technol., 6(6): pp. 518-522. https://doi.org/10.1021/es60065a006
21. Lanouette K.H., (1977). "Heavy Metals Removal", Chem. Eng., 84(21), pp. 73-80.
22. Sricharoenchaikul V., Pechyen C., Aht-ong D., Atong D. (2008) Preparation and characterization of activated carbon from the pyrolysis of physic nut (*Jatropha curcas* L.) waste, Energy Fuel, 22, pp. 31-37. https://doi.org/10.1021/ef700285u
23. Hesas R.H., Arami-Niya A., Daud W.M.A.W., Sahu J.N. (2013). Comparison of oil palm shell-based activated carbons produced by microwave and conventional heating methods using zinc chloride activation, J. Anal. Appl. Pyrolysis, 104, pp. 176-184. https://doi.org/10.1016/j.jaap.2013.08.006
24. Heidari A., Younesi H., Rashidi A., Ghoreyshi A. (2014) Adsorptive removal of CO_2 on highly microporous activated carbon prepared from Eucalyptus camaldulensis wood: effect of chemical activation, J. Taiwan Inst. Chem. Eng., 45, pp. 579-588. https://doi.org/10.1016/j.jtice.2013.06.007
25. Rojas-Mayorga C.K., Bonilla-Petriciolet A., Aguayo-Villarreal I.A., Hernández-Montoya V., Moreno-Virgen M.R., Tovar-Gómez R., M.A. Montes-Morán M.A. (2013) Optimization of pyrolysis conditions and adsorption properties of bone char for fluoride removal from water, J. Anal. Appl. Pyrolysis, 104, pp. 10-18. https://doi.org/10.1016/j.jaap.2013.09.018
26. [a]encan A., Karaboyacý M., Kýlýç M. (2015) Determination of lead(II) sorption capacity of hazelnut shell and activated carbon obtained from hazelnut shell activated with $ZnCl_{2,}$ Environ. Sci. Pollut. Res., 22, pp. 3238-3248. https://doi.org/10.1007/s11356-014-2974-9
27. Mopoung S., Moonsri P., Palas W., Khumpai S. (2015) Characterization and properties of activated carbon prepared from tamarind seeds by KOH activation for Fe(III) adsorption from aqueous solution, Sci. World J., 25, pp. 1-9. https://doi.org/10.1155/2015/415961
28. Kharrazi S.M., Mirghaffari N., Dastgerdi M.M., Soleimani M. (2020) A novel post-modification of powdered activated carbon prepared from lignocellulosic waste through thermal tension treatment to enhance the porosity and heavy metals adsorption, Powder Technology, pp. 358-368. https://doi.org/10.1016/j.powtec.2020.01.065
29. Jaramillo J., Gómez-Serrano V., Álvarez P.M. (2009) Enhanced adsorption of metal ions onto functionalized granular activated carbons prepared from cherry stones, J. Hazard. Mater., 161, pp. 670-676. https://doi.org/10.1016/j.jhazmat.2008.04.009
30. Montes-Morán M.A., Suárez D., Menéndez I.A., Fuente E. (2004) On the nature of basic sites on carbon surfaces: an overview, Carbon, 42, pp. 1219-1225. https://doi.org/10.1016/j.carbon.2004.01.023
31. Amuda O.S., Giwa A.A., Bello I.A. (2007) Removal of heavy metal from industrial wastewater using modified activated coconut shell carbon, Biochem. Eng. J., 36, pp. 174-181. https://doi.org/10.1016/j.bej.2007.02.013

32. Mojoudi N., Soleimani M., Mirghaffari N., Belver C., J. Bedia J. (2019). Removal of phenol and phosphate from aqueous solutions using activated carbons prepared from oily sludge through physical and chemical activation, Water Sci. Technol., 80, pp. 575-586. https://doi.org/10.2166/wst.2019.305

33. Schlegl H., Dawson R. (2017) Finite element analysis and modelling of thermal stress in solid oxide fuel cells, J. Power Energy, 231, pp. 654-665. https://doi.org/10.1177/0957650917716269

34. Bahtli T., Bostanci V.M., Hopa D.Y., Yasti S.Y. (2018) The effect of carbon sources on the thermal shock properties of MgO-C refractories, Universal J. Mater. Sci., 6, pp. 139-147. https://doi.org/10.13189/ujms.2018.060501

35. Hu Y.J., Chen G.Y., Ma W.C., Yan M., Han L. (2016) Distribution and contamination hazards of heavy metals in solid residues from the pyrolysis and gasification of wastewater sewage sludge, J. Residuals Sci. Technol., 13 (4), pp. 259-268. https://doi.org/10.12783/issn.1544-8053/13/4/3

36. Khallaf E.A., Authman M.M.N., Alne-na-ei A.A. (2018) Contamination and ecological hazard assessment of heavy metals in freshwater sediments and Oreochromis niloticus (Linnaeus, 1758) fish muscles in a Nile river canal in Egypt, Environ. Sci. Pollut. Res., 25 (14), pp. 13796-13812. https://doi.org/10.1007/s11356-018-1521-5

37. World Health Organization, Guidelines for drinking-water quality, Chemical Fact Sheet, World Health Organization, Geneva (2004).

38. Wang S., Peng Y. (2010) Natural zeolites as effective adsorbents in water and wastewater treatment, Chem. Eng. J., 156, p. 11"24. https://doi.org/10.1016/j.cej.2009.10.029

39. Haroun A., El-Halawany N. (2011) Preparation and evaluation of novel interpenetrating polymer network-based on newspaper pulp for removal of copper ions, Polym.-Plast. Technol., 50, pp. 232-238. https://doi.org/10.1080/03602559.2010.531435

40. Haroun A., Mashaly H., El-Sayed N. (2013) Novel nanocomposites based on gelatin/HPET/chitosan with high performance acid red 150 dye adsorption, Clean Techn. Environ. Policy, 15, pp. 367-374. https://doi.org/10.1007/s10098-012-0525-y

41. Kardam A., Raj K., Srivastava S., Srivastava M. (2014) Nanocellulose fibers for biosorption of cadmium, nickel, and lead ions from aqueous solution, Policy Clean Technol. Environ., 16, pp. 385-393. https://doi.org/10.1007/s10098-013-0634-2

42. Huang S., Song S., Zhang R., Wen T., Wang X. Yu S., *et al.,* (2017) Construction of layered double hydroxides/hollow carbon microsphere composites and its applications for mutual removal of Pb(II) and humic acid from aqueous solutions, ACS Sustain. Chem. Eng., 5, pp. 11268-11279. https://doi.org/10.1021/acssuschemeng.7b01717

43. Huang Q., Liu M., Mao L., Xu D., Zeng G., Hongye Huang, *et al.,* (2017) Surface functionalized SiO_2 nanoparticles with cationic polymers via the combination of mussel inspired chemistry and surface initiated atom transfer radical polymerization: characterization and enhanced removal of organic dye, J. Colloid Interface Sci., 499, pp. 170-179. https://doi.org/10.1016/j.jcis.2017.03.102

44. Zhang F., Song Y., Song S., Zhang R., Hou W. (2015) Synthesis of magnetite-graphene oxide-layered double hydroxide composites and applications for the removal of Pb(II) and 2,4-dichlorophenoxyacetic acid from aqueous solutions, ACS Appl. Mater. Interfaces, 16, pp. 7251-7263. https://doi.org/10.1021/acsami.5b00433

45. Gupta V.K., Imran A. (2004) Removal of lead and chromium from wastewater using bagasse fly ash-a sugar industry waste, J. Colloid Interface Sci., 27, pp. 21-28. https://doi.org/10.1016/j.jcis.2003.11.007

46. Hebeish A., Ramadan M., Abdel-Halim E., Abo-Okeil A. (2011) An effective adsorbent based on sawdust for removal of direct dye from aqueous solutions, Clean Techn. Environ. Policy, 13, pp. 713-718. https://doi.org/10.1007/s10098-010-0343-z

47. Chouchene A., Jeguirim M., Trouve G. (2014) Biosorption performance, combustion behavior, and leaching characteristics of olive solid waste during the removal of copper and nickel from aqueous solutions, Clean Techn. Environ. Policy, 16, pp. 979-986. https://doi.org/10.1007/s10098-013-0680-9

48. Wang X., Shujun Y., Chen Z., Zhao Y., Jin J., Wang X. (2017) Microstructures, and speciation of radionuclides in natural environment studied by advanced spectroscopy and theoretical calculation, Sci. China Chem., 60, pp. 1149-1152. https://doi.org/10.1007/s11426-017-9039-2

49. Li Y., Xiao H., Pan Y., Wang L. (2018) Novel composite adsorbent consisting of dissolved cellulose fiber/microfibrillated cellulose for dye removal from aqueous solution, ACS Sustain. Chem. Eng., 6, pp. 6994-7002. https://doi.org/10.1021/acssuschemeng.8b00829

50. Wang S., Peng Y. (2010) Natural zeolites as effective adsorbents in water and wastewater treatment, Chem. Eng. J., 156, p. 11"24. https://doi.org/10.1016/j.cej.2009.10.029

51. Xie Y., Changlun C., Xuemei R., Xiangxue W., Haiyan W., Xiangke W. (2019) Emerging natural and tailored materials for uranium-contaminated water treatment and environmental remediation, Mater. Sci., 103, pp. 180-234. https://doi.org/10.1016/j.pmatsci.2019.01.005

52. Wu Y., Hongwei P., Yue L., Xiangxue W., Shujun Y., Dong F., *et al.,* (2019) Environmental remediation of heavy metal ions by novel-nanomaterials: a review, Environ. Pollut., 246, pp. 608-620. https://doi.org/10.1016/j.envpol.2018.12.076

53. Rong X., Qiu F., Zhang C., Fu L., Wang Y., Yang D. (2015) Adsorption–photodegradation synergetic removal of methylene blue from aqueous solution by NiO/graphene oxide nanocomposite, Powder Technol., 275, pp. 322-328. https://doi.org/10.1016/j.powtec.2015.01.079

54. Tan P., Sun J., Hu Y., Fang Z., Bi Q., Chen Y., *et al.,* (2015) Adsorption of Cu(II), Cd(II) and Ni(II) from aqueous single metal solutions on graphene oxide membranes, J. Hazard. Mater., 297, p. 251"260. https://doi.org/10.1016/j.jhazmat.2015.04.068

55. Wang X., Shujun Y., Jin J., Wang H., Alharbi. N.S., Alsaedi A. *et al.,* (2016) Application of graphene oxides and graphene oxide-based nanomaterials in radionuclide removal from aqueous solutions, Sci. Bull., 61, pp. 1583-1593. https://doi.org/10.1007/s11434-016-1168-x

56. Kamandari H., Hashemipour H., Saeednia L., Najjarzadeh H. (2014) Experimental and modeling study on production of activated carbon from pistachio shells in rotary reactor, Res. Chem. Intermed., 40 , pp. 509-521. https://doi.or/10.1007/s11164-012-0978-y

57. Venkateswarlu S., Lee D., Yoon M. (2016) Bioinspired 2D-carbon flakes and Fe_3O_4 nanoparticles composite for arsenite removal, ACS Appl. Mater. Interfaces, 8, pp. 23876-23885. https://doi.org/10.1021/acsami.6b03583

58. Guedidi H., Reinert L., Lévêque J.M., Soneda Y., Bellakhal N., Duclaux L. (2013) The effects of the surface oxidation of activated carbon, the solution pH and the temperature on adsorption of ibuprofen, Carbon, 54, pp. 432-443. https://doi.org/10.1016/j.carbon.2012.11.059

59. Guijarro-Aldaco A., Hernández-Montoya V., Bonilla-Petriciolet A., Montes-Morán M.A., Mendoza-Castillo D.I. (2011) Improving the adsorption of heavy metals from water using commercial carbons modified with egg-shell wastes, Ind. Eng. Chem. Res., 50, pp. 9354-9362. https://doi.org/10.1021/ie2006627

60. Rong X., Qiu F., Zhang C., Fu L., Wang Y., Yang D. (2015) Adsorption–photodegradation synergetic removal of methylene blue from aqueous solution by NiO/graphene oxide nanocomposite, Powder Technol., 275, pp. 322-328. https://doi.org/10.1016/j.powtec.2015.01.079

61. Park H., Mamed N., Choo K.H. (2018) Catalytic metal oxide nanopowder composite Ti mesh for electrochemical oxidation of 1,4-dioxane and dyes, Chem. Eng. J., 345, pp. 233-241. https://doi.org/10.1016/j.cej.2018.03.158